Dettmering and Schwatke
Earth, Planets and Space (2023) 75:7
https://doi.org/10.1186/s40623-023-01764-0

Earth, Planets and Space

FULL PAPER

Open Access

Comparison of different methods to account for the plasmaspheric electron content in GNSS-derived ionospheric altimeter corrections and their impact on sea level trend estimation

Denise Dettmering* and Christian Schwatke

Abstract Global ionospheric maps based on GNSS measurements are nowadays often used to correct satellite altimeter measurements when the instruments have only one frequency or measure over coasts and inland waters. If these corrections do not account for the free electron fraction over the altimeter satellites, this leads to systematic deviations in the range measurements and thus in the estimated sea level. This study compares and assesses different approaches to reduce GNSS-based corrections for the plasmaspheric electron content. It is shown that using a simple scaling with a constant factor of 0.881 gives the best results for the Jason-1 mission, while correcting with the commonly used model ratios leads to higher sea level trend artefacts and larger noise levels, especially for periods of lower solar activity. Using this approach, the sea level trend error for both Jason-1 and Sentinel-6A can be reduced to below 0.1 mm/year, with standard deviations of the differences from the dual-frequency altimeter corrections of 6.74 mm. A simple machine learning approach (boosted regression tree) is also investigated and shows promising results. However, due to the higher processing capacity requirements and the larger deviations from long-term trend, further improvements are recommended before such an approach can be used in routine processing of altimeter corrections.

Keywords Satellite altimetry, Ionospheric delay, Plasmasphere, GIM scaling, Machine learning

*Correspondence:
Denise Dettmering
denise.dettmering@tum.de
Full list of author information is available at the end of the article

Graphical Abstract

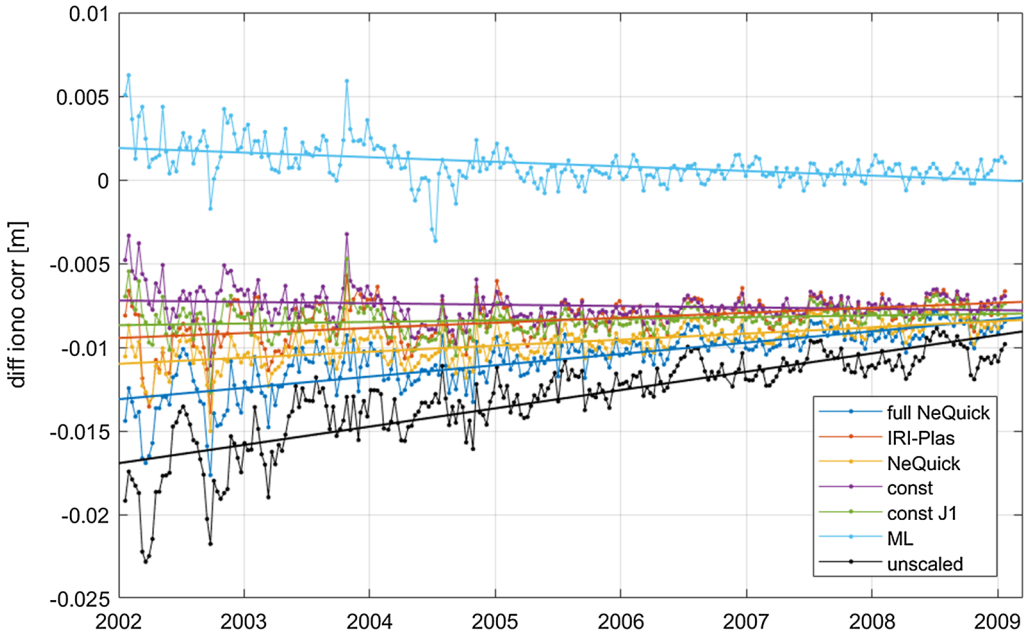

Introduction

Satellite altimetry observations need to be corrected for ionospheric delays. This is usually done by a linear combination of data measured on two different frequencies (Chelton et al. 2001). However, for some applications this approach is not recommended, and not all altimetry missions are equipped with dual-frequency instruments. In case of single-frequency altimeter instruments or for coastal or inland water applications, external model corrections are usually applied to the data (Fernandes et al. 2014).

The best external models are Global Ionospheric Maps (GIM) from Global Navigation Satellite Systems (GNSS), available from International GNSS Service (IGS) and its Analysis Centers (Hernández-Pajares et al. 2009). They provide Vertical Total Electron Content (VTEC) that can easily be converted to range corrections and interpolated to the altimetry observations. However, since the altimeter satellite orbits are much lower (about 800–1400 km altitude) than the ones of GNSS (about 20,200 km altitude), a downscaling is required to reduce the effect of free electrons above the altimeters.

Even if most of the free electrons are located in the so-called ionosphere between about 100 and 1000 km altitude, there is still a measurable impact in the so-called plasmasphere above 1300 km, i.e., the altitude of the reference altimetry missions, TOPEX/Poseidon, Jason-1 to -3, and Sentinel-6A (Yizengaw et al. 2008). The transition between ionosphere and plasmasphere is smooth and for this study the physical processes causing the delay of the microwave signals are irrelevant. Therefore, for simplicity, everything above the altimeter satellites is referred to as the plasmasphere.

GIM corrections are usually available in satellite altimetry products, the so-called Geophysical Data Records (GDR). However, since the currently applied method for scaling the GNSS data down to the orbit heights of satellite altimetry, as described in Ijima et al. (1999), is neglecting the plasmasphere above 1400 km (Dettmering and Schwatke 2022), a new approach is necessary, which can then be integrated in the processing baselines of the GDR products.

This paper builds on the previous study by the same authors (Dettmering and Schwatke 2022), in which the deficiencies of the scaling approach used so far and its effects on long-term sea level trend estimates were shown. In this follow-on study, different scaling possibilities are compared in order to identify the method that provides the most accurate results while requiring lowest processing time and effort. The focus is set to two applications: long-term sea level trends as well as scatter of the along-track residuals and their geographical patterns (in dependence to geographic latitude and local time).

The paper is structured like this: first the data and models used in the study are introduced, followed by a description of the methods applied. Afterwards, results and validation are shown before conclusions on the best approach are drawn.

Data and models

In this study, the performance of different scaling approaches for reducing GNSS VTEC to altimeter orbit height will be compared. More details on the scaling approaches are provided later in the section on methods.

This section introduces the models used in this study, i.e. the GIM models as well as the ionosphere/plasmaspheric models. Moreover, the altimetry data involved are described.

GIM models

Global ionospheric maps are provided by a variety of different institutions with different latencies, resolutions, and accuracies, and based on different input data sets (Hernández-Pajares et al. 2009).

This study is based on two types of final global maps provided by two IGS Ionosphere Associate Analysis Centers (IAACs), namely by the Jet Propulsion Laboratory JPL (JPLG) and by the Center for Orbit Determination in Europe CODE (CODG). While the JPL maps are based on a three-shell model (Mannucci et al. 1998), CODE is modelling the VTEC with spherical harmonic functions (Schaer 1999). Both maps are provided as daily files on grids of 2.5° latitude by 5° longitude with 2 h temporal resolution, and can be freely downloaded from NASA's Crustal Dynamics Data Information System CDDIS (Noll 2010) with a latency of a few days.

Ionosphere/plasmasphere models

Among the ionospheric models that contain information about the plasmasphere and that are freely available as open-source, two models are particularly widely used: the International Reference Ionosphere (IRI) and the NeQuick ionosphere electron density model.

In this study IRI-Plas 2020 (Gulyaeva and Bilitza 2012) and NeQuick2 P.531 (Nava et al. 2008) are used. Both provide electron density information globally up to GNSS altitudes of 20,200 km. While in NeQuick2 the topside model is described by a semi-Epstein layer with a height-dependent thickness parameter that is empirically determined (Chen et al. 2020), in IRI-Plas, the electron density as well as the ion density structures are modified via adapting the scale height by ingestion of 10 years of GIM-TEC data (Arikan et al. 2015). Comparisons with TEC measurements from the precise orbit determination (POD) antennae of low earth orbiting satellites (e.g., COSMIC) show that both models generally underestimate the plasmaspheric electron content between about 800–20,000 km altitude (Zhang et al. 2017; Kashcheyev and Nava 2019; Ren et al. 2020).

Altimetry data

The study is using data from the Jason-1 mission (Ménard et al. 2003), covering a period of seven years from January 2002 to January 2009. This mission is chosen since it provides data during different solar conditions covering a full spectrum from high solar activity in 2002 to low solar activity in 2009. Over the full period, the mission completed 259 repeat cycles, each one about 10 days long. For only two of these cycles (178 and 243) no data are available due to severe problems with the satellite (save hold mode). No data from the interleaved and geodetic mission phases are used in these investigations. The study makes use of the coordinates of each 1-Hz measurement as well as the related time stamps and dual-frequency ionospheric corrections.

All relevant Jason-1 altimeter data are provided in the GDR products available from AVISO+. For this study, the GDR-E version of the data is used. The ionospheric corrections are derived from a linear combination of the two carrier signals (Ku and C-Band). In order to reduce the measurement noise, an along-track smoothing of the data is recommended (Imel 1994). Usually, a filter length of about 150 km is used, however, for this application, a running median filter of about 1500 km is applied to eliminate small-scale ionospheric structures that cannot be visible in the GIM data sets.

It is important to keep in mind, that the Jason-1 mission, like all missions on the reference orbit, is nearly sun-synchronous and shows only a slow change of local time of ascending node, of about 0.2 h per day (Imel 1994; Dettmering et al. 2014). Thus, in each 10-day cycle all observations are clustered in two groups of about 2 h local time, shifted by roughly 12 h between ascending and descending passes.

In addition, data from the Sentinel-6A mission are used to prove the transferability of the results. For this purpose, the reprocessed Level 2 non-time critical high-resolution data sets from JPL's Physical Oceanography Distributed Active Archive Center PODAAC are used [named "Sentinel-6A MF Jason-CS L2 P4 Altimeter High Resolution (HR) NTC Ocean Surface Topography (Unvalidated) V2"]. The dual-frequency corrections from this product are smoothed with a 150-km median filter, since only cycle-mean ionospheric corrections are investigated.

Table 1 Scaling solutions used in this study

Solution	Scaling type	Details
0	No scaling	JPLG GIM
1	VTEC model values	JPLG GIM and NeQuick2
2	Ratio of model values	JPLG GIM and IRI-Plas 2020
3	Ratio of model values	JPLG GIM and NeQuick2
4	Const. factor	JPLG GIM and 0.881
5	Const. factor; Jason-1 period	JPLG GIM and 0.899
6	Machine learning	Regression tree

Methods

Scaling approaches

In total, seven different scaling solutions, as summarized in Table 1, are used, based on three different scaling methods: firstly, the plasmaspheric delay is added directly from a model, i.e., the NeQuick2 (1), then the scaling approach based on model ratios (relation between the model values at altimeter altitude and at GNSS altitude) published by Ijima et al. (1999) is investigated using two different ionosphere/plasmasphere models, IRI-Plas (2) as well as NeQuick2 (3). In addition, a scaling by constant factors as first suggested by Scharroo and Smith (2010) is tested. Here, two factors from Dettmering and Schwatke (2022) are applied: one estimated from more than 20 years of TOPEX and Jason data (4), and one estimated for the Jason-1 period (5). Moreover, a simple machine learning (ML) approach is tested (6), which is further explained in the next section. This not only accounts for the plasmaspheric effect, but also for the known constant offset between GIM and altimeter corrections. As a reference, the unscaled GIM correction (0) is included in the study to investigate the improvements yield by the scaling. All seven solutions are compared to the smoothed dual-frequency corrections. In contrast to solutions (1)–(3), for solutions (4)–(6) not external information from models is necessary.

Machine learning approach

In addition to model-based scaling and scaling by constant factors, a simple machine learning approach is implemented and tested for adapting the GNSS VTEC from GIM to altimetry orbit height. For this purpose a simple regression tree was chosen to fit the GIM VTEC to the smoothed dual-frequency altimeter measurements. This approach was selected because it is easy to implement (in this study predefined matlab functions are used) and, more importantly, simple to interpret (Molnar 2022).

Training data, i.e., dual-frequency altimeter corrections, are extracted from three full cycles of Jason-1 (6,104,240) in March 2002, November 2004, and July 2008. In order to reduce the input data load, only every second measurement is used. This gives a total number of 653,792 observations. Six predictors are used to fit the data. In addition to the unscaled GIM values these are: time, geomagnetic latitude, local time, month, and smoothed sunspot number R12. Geomagnetic latitude, which unlike geographic latitude refers to the geomagnetic pole rather than the geographic pole, was chosen because electrons align along magnetic field lines. The minimum number of training observations in the terminal nodes, the so-called 'minimum leaf size' is set to 2000 based on empirical tests. A smaller number improves the fitting for the cycles used for training the model while degrading the performance for most of the other cycles. With this limitation, the trained regression tree has 244 leaves, i.e., terminal nodes.

Using this model, the standard deviation of the residuals within the training data set is 1.1 cm. For those cycles, not used to train the model, the order of magnitude of the residuals is similar. However, the along-track height resolution is quite sparse, as can be seen from the yellow lines in Fig. 1. This figure shows the ionospheric corrections for two different randomly picked passes in June 2003 (cycle 52) and in January 2007 (cycle 185), which are not used for training the model. Pass 48 is overflying the Atlantic Ocean from north to south, and pass 76 is crossing the South American continent.

In order to improve the machine learning model and especially the along-track resolution of the predicted results, an ensemble of different regression trees is used, i.e. a boosted tree with 30 learners and a learning rate of 0.1. Results from this prediction are shown in red in Fig. 1 and are used for all further analyses.

One can nicely see how the fitted data (in red) now follows the level of the altimetry correction (in black and grey). Of course, differences are visible between the red and black lines, which are only partly due to the downscaling but mostly due to uncertainties of GIM models itself. One can also clearly see the data gaps in the altimetry correction due to continental overflights within pass 076, as well as the outliers of the altimetry data in coastal and polar regions (in grey) due to the long smoothing period that is no longer visible with the applied coastal and ice flagging (black lines).

By modifying the training data set and using more-advanced ML methods, the results can certainly be further improved. However, the optimization of the approach is not the focus of this work and can be dealt with in a follow-up study.

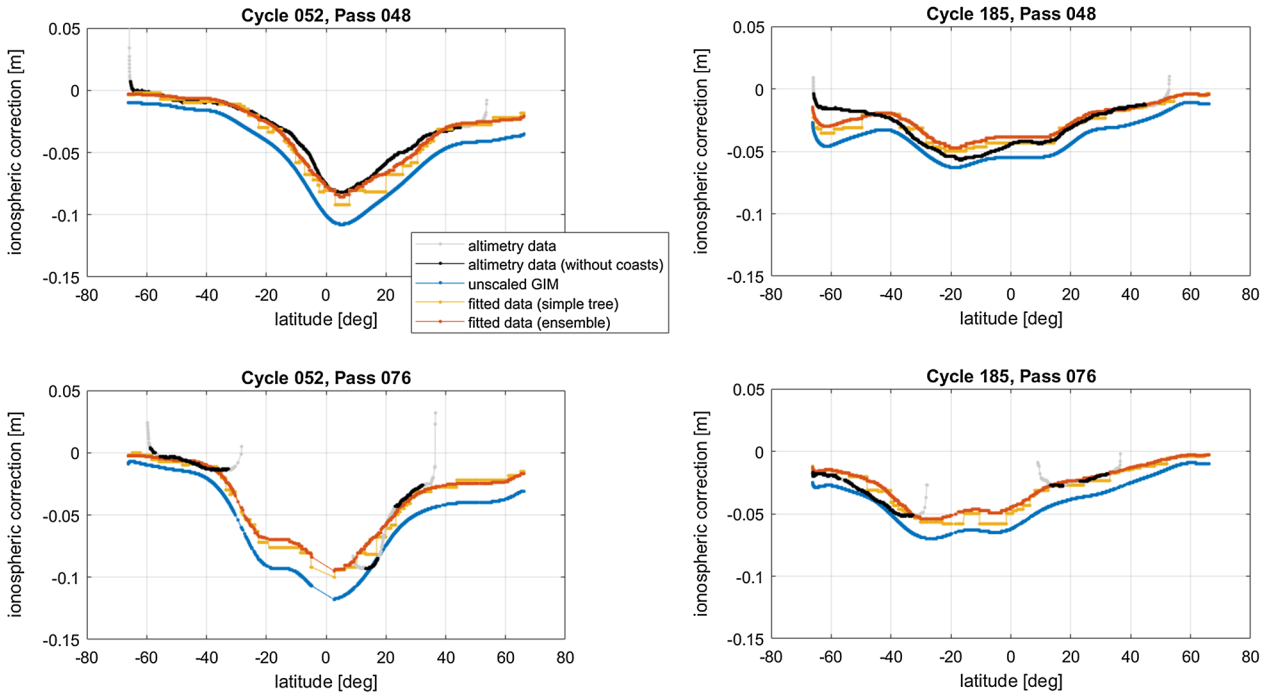

Fig. 1 Three different ionospheric corrections (unscaled GIM model in blue, dual-frequency altimeter correction in grey and black, and correction fitted by machine learning approach a simple regression tree in yellow and boosted ensemble trees in red) for four different pole-to-pole overflights (two cycles and two passes) outside the training period

Comparison strategy

For each observation of Jason-1, seven different ionospheric corrections are computed using different scaling approaches based on the JPLG GIM models. In addition, approach (3) and (0) are also applied to the CODG GIM models in order to get an idea how large the differences due to model changes are.

The smoothed dual-frequency correction is taken as trues, even it is known that it might contain a constant offset with respect to other altimetry missions and also with respect to GNSS GIMs (Azpilicueta and Nava 2021). In order to get rid of most of the small-scale effects that cannot be visible in the GIMs due to their sparse spatial resolution, the dual-frequency altimeter observations are smoothed with a median filter with a length of 100 s, i.e., about 1500 km.

Within a residual analysis for each single Jason-1 observation, differences between the smoothed dual-frequency correction and the GIM corrections (with different scalings) are computed and analysed. To present these analyses, standard deviations of the differences per 10-day Jason-1 cycle are computed, globally and for specific geomagnetic regions. Constant offsets are not analysed here, because they come mostly from the altimeter data. Changes of the offsets are analysed in the chapter on long-term trends. In order to exclude critical regions and the impact of unreliable altimeter range measurements, each observation with ocean depth smaller than 2 km (coastal areas) or sea-ice concentration larger than zero is excluded from the analyses.

As shown in Dettmering and Schwatke (2022), an inadequate scaling of VTEC can lead to severe long-term trend differences in ionospheric corrections and thus in sea level variation. In order to investigate the effects of different scaling approaches to sea level trends, the trend differences of the generated corrections is analysed. For that purpose, for each cycle all ionospheric corrections are averaged per scaling solution and the mean from the dual-frequency corrections is subtracted. For trend analyses only data collected in geographic latitudes between $\pm 55°$ are used in addition to the outlier criteria mentioned above.

Results

Figure 2 shows the plasmaspheric part of the ionospheric correction as derived by three different scaling approaches (2, 3, 4) for Jason-1 Cycle 015 (June 2002; high solar activity; local time of descending/ascending passes = 19.7/6.2 h). One can clearly see the higher values for late afternoon (descending passes) than for early morning (ascending passes), even if the order of magnitude is quite similar, since in both cases the

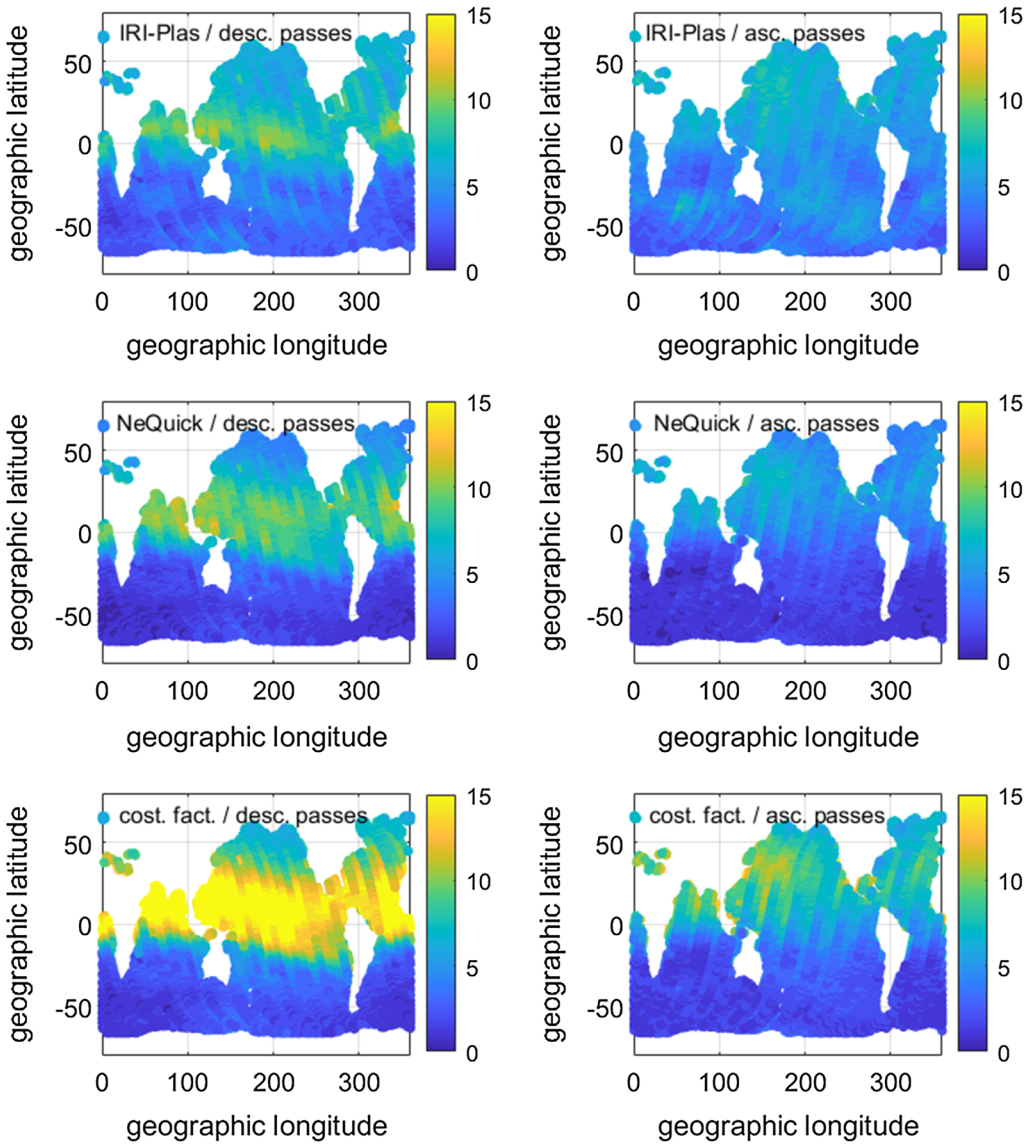

Fig. 2 Plasmaspheric part of scaled ionospheric correction for Jason-1 Cycle 015 for three different scaling approaches (top: IRI-Plas ratio; middle: NeQuick ratio; bottom: constant factor) and separately for descending passes (left-hand side) and ascending passes (right-hand side). Colours indicate differences between scaled range delays and unscaled range delays in mm

maximum solar activity shortly after noon is missed. The largest values, up to about 2 cm are reached in low latitudes around the geomagnetic equator. Moreover, clear differences between the three different scaling solutions are visible, with much larger values for the constant factor solution (4; bottom), than for the other two solutions. In addition, the IRI-scaled solution (2; top) only shows one latitude band for the descending passes, whereas for the NeQuick-scaled solution (3; middle) two bands north and south of the geomagnetic equator are visible.

This example already shows that significant differences between the different scaling approaches exist. To check which of the scaling solutions provides the best results, a comparison to the dual-frequency altimetry data is done, and the validation results are presented in the following section.

Residual analysis

For each single altimetry observation, the difference in ionospheric correction between the GIM-based solutions (with the different scaling approaches) and the smoothed

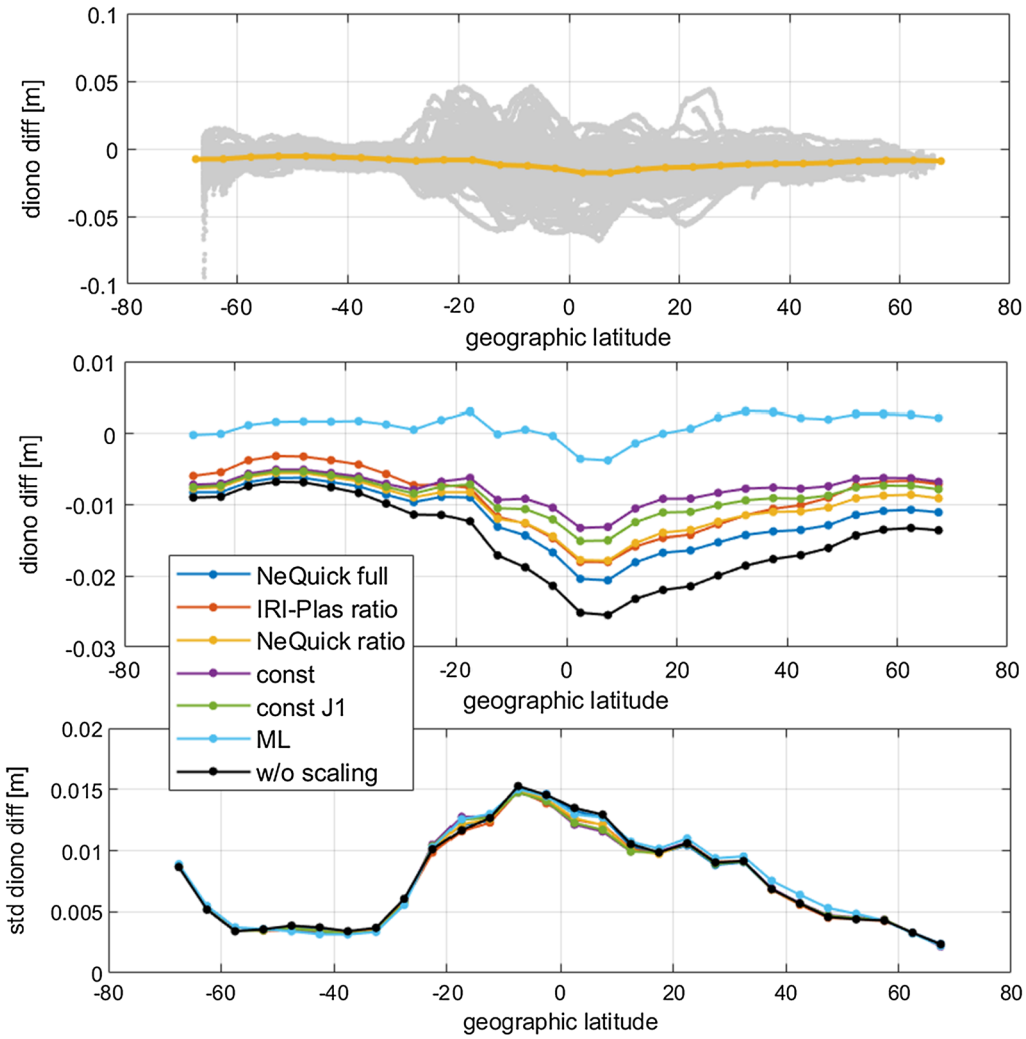

Fig. 3 Differences (diff) in ionospheric corrections (diono) with respect to smoothed dual-frequency correction for Jason-1 Cycle 015 (June 2002). Top plot shows the differences from the solution scaled with NeQuick ratio (3) in grey and the median for 5-degree latitude classes. The middle plot shows the median differences for all seven solutions and the bottom plot the respective standard deviation (std) per latitude class

dual-frequency correction is computed. The top plot in Fig. 3 shows the differences of solution 3 (scaled with NeQuick ratio) for Jason-1 Cycle 015 in dependence from geographical latitude. One can see that for lower latitudes the scatter of differences as well as their median values (orange line) are largest. The middle plot shows the median values per 5-degree latitude class for all seven solutions, the bottom plot the respective standard deviations. While only slight differences between the standard deviations are visible, mainly in the low latitudes, systematic differences in the median values are visible. One can nicely see how each of the solutions improves the latitude dependency of the unscaled version (black). In fact, the solutions mostly differ in offset (which is known to exist in the altimetry data). Only the IRI-Plas solution (2, red) show a different shape than the other scaled solutions with more remaining latitude dependency. Since the ML solution (6) is trained with the dual-frequency corrections, the offset is removed within the scaling process.

As this example shows, the noise within one cycle is larger than the systematic latitudinal effects. Consequently, in the following only the standard deviations of residuals will be further investigated based on the full data set.

As shown in the example above and as commonly known, the performance of every electron density model strongly depends—among other factors—on geomagnetic latitude and solar activity. Thus, the residual

analyses shown here are performed for different latitude bands, namely for low latitudes (between ±25° geomagnetic latitude), mid-latitudes (between 25° and 45° N/S), and high latitudes (above 45° N and S). This classification follows Yizengaw et al. (2008). Another important factor impacting the ionospheric corrections is the solar activity varying with a period of about 11 years. This can be quantified by the solar flux or the number of sunspots. In this study, the 12-month running mean of sunspot number R12 (ITU 1999) is used to separate between low (R12 < 30) and high (R12 > 30) solar activity. This threshold, reached in April 2005, ensures a similar number of Jason-1 cycles for low (136) and high (121) solar activity.

Table 2 lists the standard deviations for different latitude classes and for low and high solar activity, respectively. The first row shows the mean global standard deviations for the full Jason-1 period. For a more easy interpretation, the same results are illustrated in Fig. 4, but relative to the unscaled GIM solution and in percentage. A positive value indicates the improvement by the scaling with respect to the original unscaled GIM correction. It can be seen that all solutions improve the consistency to dual-frequency altimetry corrections, with only one exception: the machine learning approach slightly degrades the correction for high solar activities in high latitudes by about 1%. All other values indicate improvements between about 2 and 17%.

When comparing solution (1) and (3), it becomes clear that it is recommended to use the ratio from the models instead of its full VTEC values, even with a quite good performing model like NeQuick. In fact, NeQuick outperforms IRI-Plas for almost all regions: only for high solar activity and in low latitudes, IRI slightly outperforms NeQuick. However, for most data classes, the usage of simple constant scaling factors works better or very similar to the scaling by plasmaspheric models. Only for low latitudes under high solar activity the model-ratio scaling outperforms constant factors. When comparing the different factors, i.e. solution (4) and (5), it becomes clear that the specific factor for the Jason-1 period, works better for high solar activity but worse in case of low solar activity. Overall, the more general factor outperforms the mission-specific one.

Table 2 Mean standard deviation of differences to dual-frequency correction for different regions (LL: low latitudes; LM: mid-latitudes; LH: high latitudes) and solar activity (SH: high solar activity; SL: low solar activity) and for all Jason-1 data (all/global); all numbers in mm; best solution in bold

Solution	All/global	SH/LL	SH/LM	SH/LH	SL/LL	SL/LM	SL/LH
0	7.67	12.43	7.16	6.11	6.40	4.20	4.26
1	7.16	12.20	6.78	5.95	5.93	3.96	4.18
2	7.23	**11.91**	6.92	6.05	6.00	3.97	4.04
3	6.99	11.93	6.72	**5.93**	5.76	3.85	4.09
4	6.74	12.05	6.71	5.96	**5.43**	3.68	**4.01**
5	6.80	11.96	**6.68**	**5.93**	5.52	3.73	4.04
6	**6.72**	12.14	6.88	6.20	5.44	**3.48**	**4.01**

The bold numbers indicate the best solutions

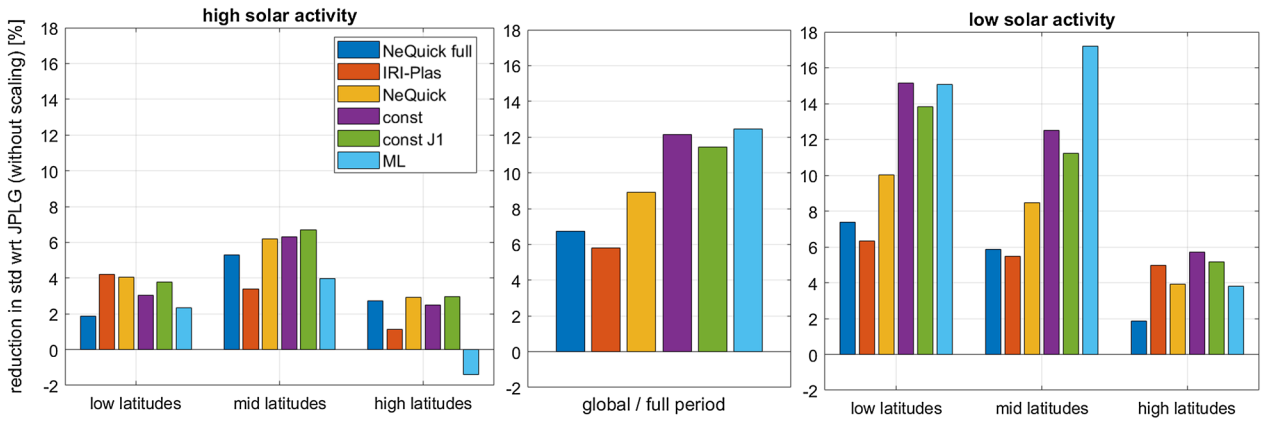

Fig. 4 Mean standard deviations for different scaling solutions, in different regions and for different solar activities. Shown is the improvement with respect to unscaled GIM in percent

What is important to keep in mind is that most part of the residuals are not stemming from the scaling approach, but from the differences between the GIM models and the dual-frequency corrections, i.e. mainly from uncertainties of the GNSS modelling in the ocean regions that are only sparsely covered by measurements. A comparison with an alternative GIM is shown later to give an idea on the impact of the underlying GIM model on the residuals. Moreover, due to the significant smoothing of the along-track altimetry data (see "Data and models" section), the standard deviations shown here are not describing the full uncertainties of the GIM models, but can only be used to compare the performance of the different scaling approaches.

To better understand the parameters influencing the scaling performances, the temporal behaviour of standard deviation differences is analysed. This is only done for three different pairs of solutions, including the four most promising scaling solutions (2–5).

The top plot of Fig. 5 shows the comparison of the best model-ratio scaling (NeQuick) with the best constant factor scaling (const). One can see that the scaling by using the model produces better or similar results for high solar activity, especially for low latitudes, whereas for low solar activity the factor-scaling performs better for all latitude classes. Also visible is a dependency on season (higher improvements for constant scaling in summer months) and on the local time of the measurement, related to the Jason-1 orbit. Here, the largest improvements are to be detected when either the descending or the ascending passes are measured around about 2–3 pm local time (peaks in the red time series).

The second comparison, shown in the middle plot of Fig. 5, is between the two different constant scaling factors. The differences are much smaller here, but show a similar behaviour: the long-term constant factor

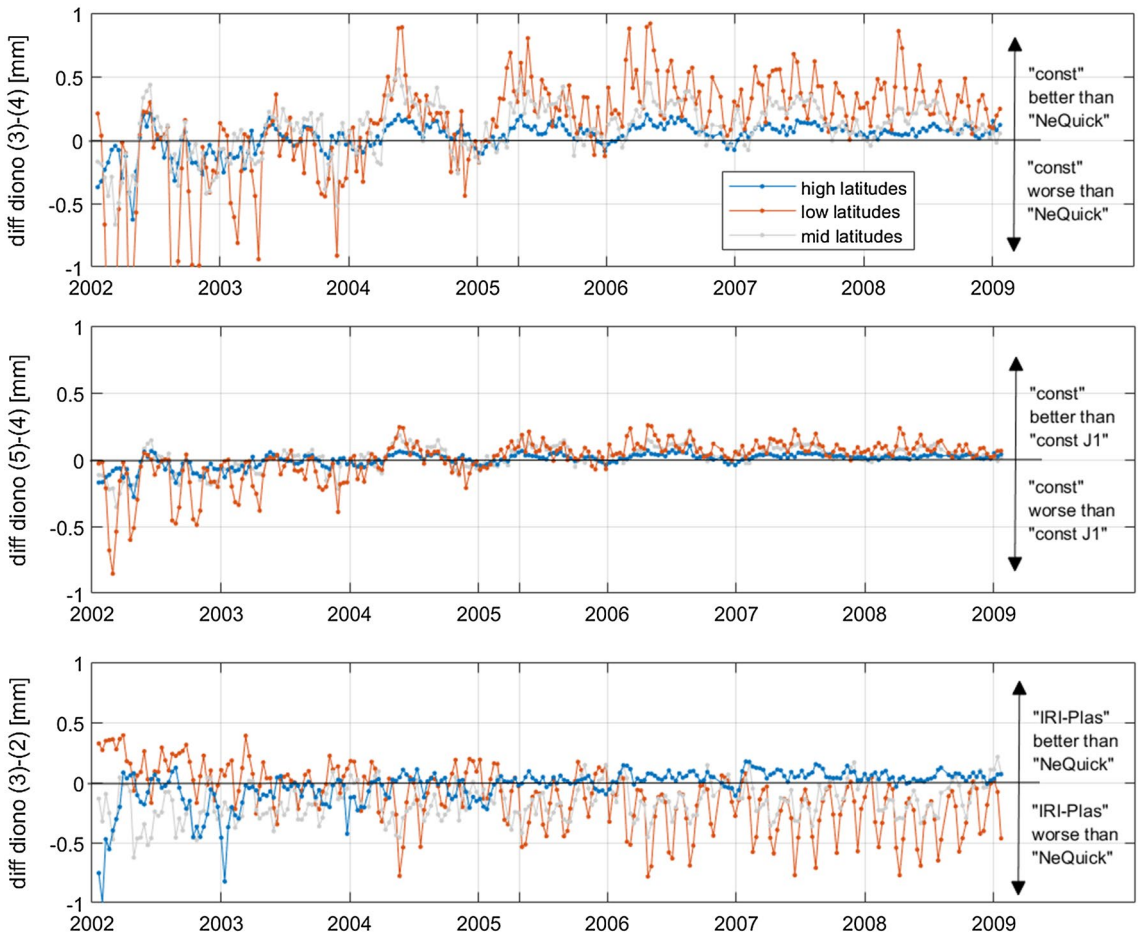

Fig. 5 Difference of standard deviations per Jason-1 cycle between constant scaling and scaling by NeQuick ratio (top plot), constant scaling by different factors (middle), and between IRI-Plas and NeQuick scaling. The standard deviations are computed for different classes of geomagnetic latitude (low: red, high: blue, mid: grey). The grey line in April 2005 indicates the change from high solar activity to low solar activity (R12 = 30)

performs better for lower solar activity and for the high latitude region.

In the bottom plot of Fig. 5, the two different models are compared: NeQuick and IRI-Plas. Here, the dependence on local time of observations is clearly visible, and significantly degrades the performance of the IRI-scaling in low latitudes for about six cycles per year. In these differences, no seasonal signal can be detected, thus, it seems that both models handle seasonal effects equally.

Impact on long-term trends

At least as important as the small-scale and along-track accuracy of the scaling approaches is the long-term consistency. As shown by Dettmering and Schwatke (2022), the choice of ionospheric corrections for satellite altimetry has significant impact on the estimated global mean sea level trends. As reported there, the usage of unscaled GIM correction leads to about 1 mm/year change in estimated sea level trend for Jason-1.

Here, it is investigated how well the different scaling approaches are able to reduce these trend errors that map directly in sea level rise estimates. The results are shown in Fig. 6 and are summarized in Table 3. Each of the scaling approaches is able to reduce the trend difference with respect to the altimetry-derived ionospheric correction. When relying to NeQuick it is better to use the VTEC ratio for scaling than the VTEC values itself. In terms of trend, the IRI-Plas scaling works better than NeQuick, even if the estimation is noisier. Best long-term consistency to the altimetry data is reached with the constant scaling approaches. Both factors end up with very similar trend differences (one negative, one positive), both below 0.1 mm/year in absolute trend difference with respect to the altimetry time series. The machine learning approach yields a trend difference of about 0.3 mm/year. However, most of this difference seems to be related to the first 2.5 years, while the time series looks quite stable after about mid-2004. This finding suggests that there is still room for improvement of the ML approach, e.g., by adding more training data from high solar activity periods.

Table 3 Differences in trend with respect to dual-frequency altimetry data

Solution	Scaling type	Trend differences [mm/year]	Std of differences [mm]
0	Unscaled	1.095 ± 0.045	2.7
1	NeQuick VTEC	0.677 ± 0.033	1.7
2	IRI ratio	0.297 ± 0.034	1.3
3	NeQuick ratio	0.362 ± 0.025	1.1
4	Const	-0.082 ± 0.028	0.9
5	Const J1	0.096 ± 0.025	0.8
6	ML	-0.275 ± 0.033	1.2

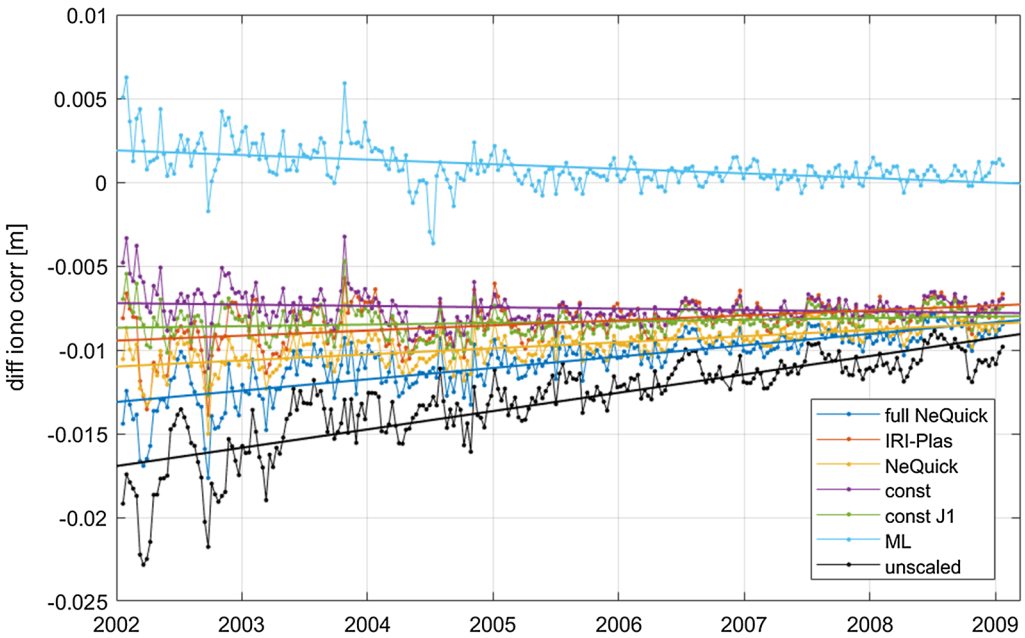

Fig. 6 Trend differences to smoothed dual-frequency altimeter for different scaling solutions

At this point it should be pointed out again that the two-frequency altimeter measurements are assumed to be stable over time and to have no trend. If this assumption is not correct, the trend differences here only show the degree of consistency with the altimetry and cannot be regarded as absolute errors.

Impact of underlying GIM product type

All results presented until now are based on the GIMs from JPL, i.e., the JPLG maps. Today, many other global VTEC maps exist, which show different performance when compared to dual-frequency altimetry data (Hernández-Pajares et al. 2009). From the many alternative products, the CODG maps are selected here to show the influence of the underlying GIM on the results. To test more or all of the existing product is outside the scope of this paper. Both products (JPLG and CODG) are scaled by NeQuick ratio (solution 3), since this solution shows better results than solutions 1 and 2. Solutions 4 and 5 cannot be used, as the applied constant factors were derived from JPLG (Dettmering and Schwatke 2022), which might bias the results.

The mean standard deviations of the residuals change by up to about 2 mm when switching from JPLG to CODG. This is more than 30% of the full standard deviation (for mid and high latitudes, relative to JPLG standard deviation). In general, CODG shows larger discrepancies to the dual-frequency observations than JPLG, especially for high solar activities as visible from Fig. 7. Only for low solar activity and in low latitudes, the unscaled CODG solution outperforms JPLG in terms of mean standard deviations. The figure also makes clear that underlying GIM model has a similar (for low solar activities) or even larger (for high solar activities) impact on the consistency to dual-frequency altimetry corrections than the scaling itself (and even more than the usage of different scaling solutions).

The model switch is also visible in the trend analysis—although in this case, the effect is smaller than that due to the scaling itself. When using CODG maps, the trend differences with respect to dual-frequency observations increase from 0.36 mm/year to 0.46 mm/year. This difference of about 0.1 mm/year is already visible in the unscaled solutions (1.1–1.2 mm/year) and does not change with the scaling (Fig. 8).

Transferability to Sentinel-6A

All investigations presented until now have been based on the Jason-1 mission. It is assumed that the results can be safely transferred to other missions following the same orbit, since a full range of different ionospheric activities and seasons is covered in this data set. Nevertheless, it should be checked, how the performance in terms of long-term stability for the Sentinel-6 mission is, which was launched in November 2020 (Donlon et al. 2021). Sentinel-6A Michael Freilich, formerly also known as Jason-CS, is part of the Copernicus Programme and is a result of international cooperation between ESA, EUMETSAT, European Union, NOAA, CNES and NASA/JPL. Since April 2022, Sentinel-6A has replaced Jason-3 as the ocean surface topography reference mission.

Figure 9 shows the long-term evolution of ionospheric corrections over the lifetime of Sentinel-6 from late 2020

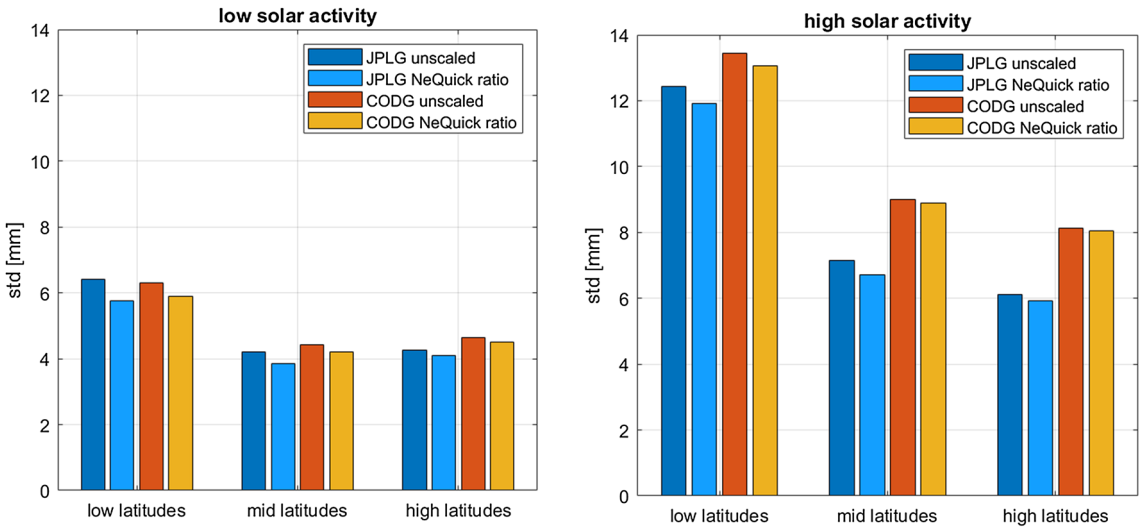

Fig. 7 Standard deviations of the differences of GIM solutions with respect to smoothed dual-frequency altimeter corrections for different solar activities (left: low; right: high) and different geomagnetic latitude classes

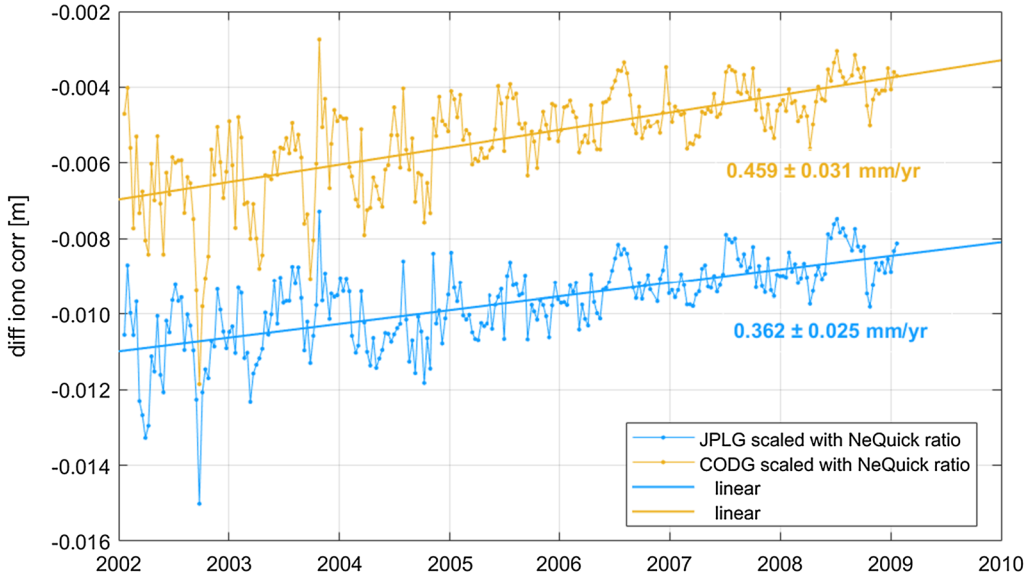

Fig. 8 Trend differences to smoothed dual-frequency altimeter for two different GIM types (JPLG in blue and CODG in orange); both scaled with NeQuick ratio (solution 3)

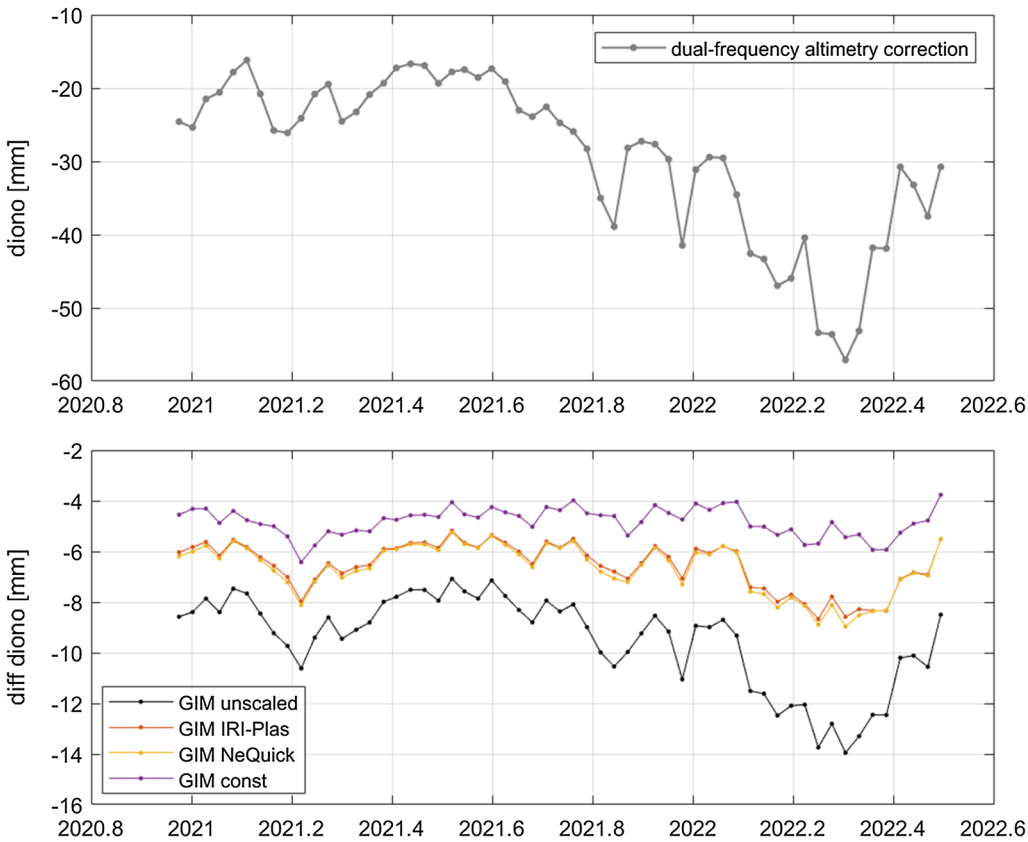

Fig. 9 Ionospheric corrections for Sentinel-6A. Top plot: dual-frequency altimeter correction, bottom plot: four GIM-based corrections based on different scaling approaches; differences with respect to dual-frequency altimeter corrections

until mid 2022 (about 1.5 years). After the launch of Sentinel-6A, the solar activity that reached a minimum in early 2020 started growing again. This can also be seen in the evolution of the mean ionospheric correction per cycle that is illustrated in the top plot. Towards the end of the time series, a degradation in absolute ionospheric correction can be seen again. The unscaled GIM correction is impacted by this behaviour, as visible in the bottom plot of Fig. 9 showing the differences to the dual-frequency altimeter correction. All three scaling solution shown in this plot can reduce the systematic effect, with the best performance for the scaling by constant factor 0.881. When computing linear trends of these differences (even if it is obvious that the behaviour is not linear), one ends up with −2.6 mm/year for the unscaled GIM solution, −1.0 mm/year for both model corrections, and −0.1 mm/year for the constant factor scaling. The different offsets visible are due to a bias in the Sentinel-6A corrections, which reaches about 4 mm.

This proves that the constant scaling factor of 0.881 as estimated by Dettmering and Schwatke (2022) can safely be applied to all altimeter missions flying on the references orbit. For altimeter orbiting in other altitudes, such as Sentinel-3 or Saral, dedicated scaling factors must be derived.

Conclusion

This study compares seven GIM-derived ionospheric altimeter corrections based on different approaches to account for the plasmaspheric electron content above the altimeter satellite. The accuracy of the different scaling approaches is assessed by comparison with dual-frequency altimeter corrections. As to be expected, the performance strongly depends on solar activity, geomagnetic latitude and local time of observations.

The following main conclusions can be drawn from the comparisons:

- When using a model for accounting for the plasmaspheric electron content, model ratios between the two orbit heights involved should be preferred instead of the model values themselves.
- NeQuick ratios perform better than IRI-Plas ratios, except for low latitudes during high solar activity. Due to the degraded performance of NeQuick scaling under these conditions, IRI-Plas can reduce the long-term trend differences with respect to dual-frequency altimetry corrections slightly better (by 0.06 mm/year) than NeQuick.
- Even if the choice of the underlying GIM is strongly influencing the residuals with respect to dual-frequency altimeter observations, the impact on sea level trend estimation is minor. For the Jason-1 period, the difference between JPLG and CODG, both scaled with NeQuick ration, is about 0.1 mm/year.
- In terms of residuals, the scaling by constant factors outperform the models for almost all regions and conditions. Only for low latitudes and high solar activity, the models perform slightly better. For trend differences, the factor approach is about three times better than the model ratios.
- When comparing both factors under investigation, the long-term factor performs better for low solar conditions, whereas the factor estimated from Jason-1 only, produces better results for high solar activities. In terms of long-term trends, very similar performance is reached for both factors.
- The machine learning approach shows similar performance than the scaling using models or empirical factors, but with large performance differences. Over all regions and activities investigated, the standard deviation of residuals is smallest for this approach. However, for high solar activity and high latitudes, the performance is even worse than without any scaling. In terms of trend differences, the machine learning solution performs similar than the two model-ratio approaches.

What is important to note is that these results do not allow for a conclusion regarding the absolute quality of the ionosphere models NeQuick and IRI-Plas, since only the ratio of the VTEC values at two different altitudes is used. Moreover, the better performance of the constant factors may come from the fact that they were optimized for this particular application and the altimeter data itself was used for their calculation.

In summary, the application of a long-term constant factor for scaling the GIM solutions to satellite altimetry orbit height is recommended. When taking all Jason-1 observations into account, this approach works best in terms of residuals and trends with respect to dual-satellite altimetry corrections. Moreover, it is easier to apply and significant faster than all other approaches. Since a dedicated Jason-1 scaling factor is not systematically better than the factor estimated from long-term data of TOPEX, Jason-1, Jason-2, and Jason-3, the long-term factor of 0.881 as estimated by Dettmering and Schwatke (2022) is recommended. This scaling factor can also be consistently applied to the other Jason missions as well as to Sentinel-6.

The presented machine learning approach is of higher complexity than using constant scaling factors. In addition, the results are less easy to interpret. Thus, even if

the validation results are promising, before any routine application to altimetry data products, a more detailed study is recommended.

Finally, it should be noted that the selection of the most appropriate approach is based on the assumption that the altimeter-derived ionospheric corrections are free of systematic errors and especially without long-term drift behaviour. If this is not the case, the GIM scaling by a constant scaling factor is the solution with the best consistency to the two-frequency measurements—but not necessarily the best solution in terms of unbiased absolute sea level trends.

This study addresses Jason-1 and can be directly applied to the other missions on the reference orbit. The scaled GIM corrections are mainly applicable for inland and coastal areas. For missions operating at other altitudes (especially those with only one altimeter frequency such as Cryosat-2 or SARAL) the model-based scaling methods can be transferred directly. In contrast, the constant scaling factors must be derived separately for each orbit altitude, preferably from measurements of two-frequency missions on similar orbits.

Acknowledgements
The authors thank the agencies in charge for the altimetry satellites and data, especially AVISO for providing access to the Jason-1 GDR data. The GIM were obtained through the online archives of the Crustal Dynamics Data Information System (CDDIS), NASA Goddard Space Flight Center, Greenbelt, MD, USA. Many thanks also to IGS for setting up and maintaining the infrastructure for generating the global GIMs. We also want to thank Yenca Migoya-Orue and colleagues for providing the NeQuick2 software and instructions on how to get it running. Many thanks also to the IRI-Plas team for freely providing the source code of this model.

Author contributions
DD designed the study, performed the computations and analyses and wrote the manuscript. CS was responsible for the altimetry database organization. Both authors read and approved the final manuscript.

Funding
Open Access funding enabled and organized by Projekt DEAL.

Availability of data and materials
The Jason-1 used within this study is taken from AVISO (https://www.aviso.altimetry.fr). Sentinel-6A data is available from https://podaac.jpl.nasa.gov/dataset/JASON_CS_S6A_L2_ALT_HR_STD_OST_NTC_F_UNVALIDATED_V2 (doi:10.5067/S6AP4-2HSNUR; last access: August 30, 2022). Jason-1 dual-frequency VTEC data can be found at OpenADB (https://openadb.dgfi.tum.de/en/products/vertical-total-electron-content/). The GIM models were obtained through the online archives of the Crustal Dynamics Data Information System (CDDIS), NASA Goddard Space Flight Center, Greenbelt, MD, USA (https://cddis.nasa.gov/archive/gnss/products/ionex/). IRI-Plas software is provided at the website of the Pushkov Institute of Terrestrial Magnetism, Ionosphere and Radio Wave Propagation (IZMIRAN) at https://ftp.izmiran.ru/pub/izmiran/SPIM/ (last access: August 29, 2022). The source code of NeQuick 2 model is distributed by the Ionosphere Radiopropagation Unit of the T/ICT4D Laboratory on request (https://t-ict4d.ictp.it/nequick2/source-code).

Declarations

Competing interests
The authors declare that they have no competing interests.

Author details
[1]Deutsches Geodätisches Forschungsinstitut (DGFI-TUM), Technical University of Munich, Munich, Germany.

Received: 17 September 2022 Accepted: 1 January 2023
Published online: 18 January 2023

References

Arikan F, Sezen U, Gulyaeva T et al (2015) Online, automatic, ionospheric maps: IRI-PLAS-MAP. Adv Space Res 55(8):2106–2113. https://doi.org/10.1016/j.asr.2014.10.016

Azpilicueta F, Nava B (2021) On the TEC bias of altimeter satellites. J Geod. https://doi.org/10.1007/s00190-021-01564-y

Chelton D, Ries J, Haines B et al (2001) Satellite altimetry and earth sciences. A handbook of techniques and applications. In: Fu L-L, Cazenave A (eds) Satellite altimetry. Academic Press, Cambridge

Chen J, Ren X, Zhang X et al (2020) Assessment and validation of three ionospheric models (IRI-2016, NeQuick2, and IGS-GIM) from 2002 to 2018. Space Weather 18(6):e2019SW002,422. https://doi.org/10.1029/2019SW002422

Dettmering D, Schwatke C (2022) Ionospheric corrections for satellite altimetry—impact on global mean sea level trends. Earth Space Sci 9(4):e2021EA002,098. https://doi.org/10.1029/2021EA002098

Dettmering D, Limberger M, Schmidt M (2014) Using DORIS measurements for modeling the vertical total electron content of the Earth's ionosphere. J Geod 88(12):1131–1143. https://doi.org/10.1007/s00190-014-0748-2

Donlon CJ, Cullen R, Giulicchi L et al (2021) The Copernicus Sentinel-6 mission: enhanced continuity of satellite sea level measurements from space. Remote Sens Environ 258(112):395. https://doi.org/10.1016/j.rse.2021.112395

Fernandes M, Lázaro C, Nunes A et al (2014) Atmospheric corrections for altimetry studies over inland water. Remote Sens 6(6):4952–4997. https://doi.org/10.3390/rs6064952

Gulyaeva T, Bilitza D (2012) Towards ISO standard earth ionosphere and plasmasphere model. In: Larsen R (ed) New developments in the standard model. Nova Science Publishers, Hauppauge, pp 1–39

Hernández-Pajares M, Juan JM, Sanz J et al (2009) The IGS VTEC maps: a reliable source of ionospheric information since 1998. J Geod 83(3–4):263–275. https://doi.org/10.1007/s00190-008-0266-1

Ijima B, Harris I, Ho C et al (1999) Automated daily process for global ionospheric total electron content maps and satellite ocean ionospheric calibration based on Global Positioning System. J Atmos Solar Terr Phys 61(16):1205–1218. https://doi.org/10.1016/S1364-6826(99)00067-X

Imel DA (1994) Evaluation of the TOPEX/POSEIDON dual-frequency ionosphere correction. J Geophys Res Oceans 99(C12):24895–24906. https://doi.org/10.1029/94JC01869

ITU (1999) Choice of indices for long-term ionospheric predictions. Recommendation ITU-R P.371-8, https://www.itu.int/rec/R-REC-P.371-8-199907-I/en. Accessed 01 Sept 2022

Kashcheyev A, Nava B (2019) Validation of NeQuick 2 model topside ionosphere and plasmasphere electron content using COSMIC POD TEC. J Geophys Res Space Phys 124(11):9525–9536. https://doi.org/10.1029/2019JA026971

Mannucci AJ, Wilson BD, Yuan DN et al (1998) A global mapping technique for GPS-derived ionospheric total electron content measurements. Radio Sci 33(3):565–582. https://doi.org/10.1029/97RS02707

Ménard Y, Fu LL, Escudier P et al (2003) The Jason-1 mission special issue: Jason-1 calibration/validation. Mar Geod 26(3–4):131–146. https://doi.org/10.1080/714044514

Molnar C (2022) Interpretable machine learning: a guide for making black box models explainable. https://christophm.github.io/interpretable-ml-book/. Accessed 16 Sept 2022

Nava B, Coïsson P, Radicella S (2008) A new version of the NeQuick ionosphere electron density model. J Atmos Solar Terr Phys 70(15):1856–1862. https://doi.org/10.1016/j.jastp.2008.01.015

Noll CE (2010) The crustal dynamics data information system: a resource to support scientific analysis using space geodesy. Adv Space Res 45(12):1421–1440. https://doi.org/10.1016/j.asr.2010.01.018

Ren X, Chen J, Zhang X et al (2020) Topside ionosphere of NeQuick2 and IRI-2016 validated by using onboard GPS observations from multiple LEO satellites. J Geophys Res Space Phys 125(9):e2020JA027,999. https://doi.org/10.1029/2020JA027999

Schaer S (1999) Mapping and predicting the Earths ionosphere using the global positioning system. Ph.D. Thesis. University of Bern

Scharroo R, Smith WHF (2010) A global positioning system-based climatology for the total electron471content in the ionosphere. Journal of Geophysical Research 115(A10318).472. https://doi.org/10.1029/2009JA014719

Yizengaw E, Moldwin M, Galvan D et al (2008) Global plasmaspheric TEC and its relative contribution to GPS TEC. J Atmos Solar Terr Phys 70(11–12):1541–1548. https://doi.org/10.1016/j.jastp.2008.04.022

Zhang ML, Liu L, Wan W et al (2017) Comparison of the observed topside ionospheric and plasmaspheric electron content derived from the COSMIC podTEC measurements with the IRI_Plas model results. Adv Space Res 60(2):222–227. https://doi.org/10.1016/j.asr.2016.10.025

Publisher's Note